Usnic Acid Induces Cycle Arrest, Apoptosis, and Autophagy in Gastric Cancer Cells *In Vitro* and *In Vivo*

Authors' Contribution:
Study Design A
Data Collection B
Statistical Analysis C
Data Interpretation D
Manuscript Preparation E
Literature Search F
Funds Collection G

ABCDEF 1 **Xiaoge Geng**
BDE 1 **Xing Zhang**
BDF 1 **Bin Zhou**
CE 2 **Chenjing Zhang**
AC 2 **Jiangfeng Tu**
AD 1 **Xiaojun Chen**
BC 1 **Jingya Wang**
BC 2 **Huiqin Gao**
CF 3 **Guangming Qin**
ACG 1,4 **Wensheng Pan**

1 Department of Gastroenterology, The Second Affiliated Hospital, School of Medicine, Zhejiang University, Hangzhou, Zhejiang, P.R. China
2 Department of Gastroenterology and Endoscopy Center, Zhejiang Provincial People's Hospital, Hangzhou, Zhejiang, P.R. China
3 Department of Laboratory, The Second Affiliated Hospital, School of Medicine, Zhejiang University, Hangzhou, Zhejiang, P.R. China
4 Department of Gastroenterology and Endoscopy Center, Zhejiang Provincial People's Hospital, People's Hospital of Hangzhou Medical College, Hangzhou, Zhejiang, P.R. China

Corresponding Authors: Wensheng Pan, e-mail: pan2010@zju.edu.cn; wspan223@163.com
Source of support: This work was supported by the National Natural Science Foundation of China (general project No. 81372302) and the Key Project of Zhejiang Province (No. 2013C03044-5)

Background: Usnic acid (UA), a secondary metabolite, is mainly derived from certain lichen species. Growing evidence suggests that UA has antitumor, anti-oxidative, anti-inflammatory, and other activities in a variety of cancer cells. However, the antitumor effect of UA in gastric cancer cells (GC) is unclear. The aim of this investigation was to assess the antitumor effect of UA in GC cells *in vitro* and *in vivo*, and to explore the underlying mechanisms.

Material/Methods: Cell proliferation was measured by CCK8 assay, the arrest of cell cycle was assessed by flow cytometry, and cellular apoptosis was observed via Hoechst 33258 staining assay. Expression levels of apoptosis-related proteins (activated caspase-3 and PARP, Bax, Bcl2) and autophagy-associated proteins (LC3-II and p62) were verified through Western blot analysis. H&E staining and immunohistochemistry were carried out in the subcutaneously implanted BGC823 tumor model in a nude mouse experiment.

Results: *In vitro*, we demonstrated that UA was significantly effective in inducing morphological changes, inhibiting the cell proliferation dose- and time-dependently, arresting the cell cycle phase, promoting cancer cellular apoptosis, and inducing autophagy activity. *In vivo*, compared to mice treated with 5-FU alone, UA treatment was significantly more effective in suppressing the tumor growth without affecting body weight, and in regulating the amount of Bax and Bcl2 in tumor tissues.

Conclusions: UA induces cell cycle arrest and autophagy and exerts anti-proliferative and apoptotic effects by modulating expression of apoptosis-related proteins in stomach neoplasm cells, and has a better antitumor effect compared to 5-Fu in the xenograft model.

MeSH Keywords: Apoptosis • Autophagy • Cell Cycle • Stomach Neoplasms • Usnea • Xenograft Model Antitumor Assays

Full-text PDF: https://www.medscimonit.com/abstract/index/idArt/908568

📄 3997   🗄 —   📊 4   📚 40

Background

According to the Global Cancer Statistics of 2012, Gastric cancer is the fourth and the fifth most frequently diagnosed cancer and the third and the fifth leading cause of cancer-related death in men and women, respectively, worldwide [1]. In recent years, stomach cancer incidence has been declining in areas with historically high rates, but incidence rates are still high in China [1]. Surgery, as a primary treatment of choice for patients with GC, often is ineffective because many GC patients already have locally advanced or metastatic cancer disease at primary diagnosis, as well as due to recurrence after complete surgical resection, resulting in high GC mortality rates worldwide [2,3]. Chemotherapy, a conventional treatment strategy for metastatic GC, includes fluoropyrimidines, administered alone or in combination, such as with 5-fluorouracil (5-FU), capecitabine, and S-1, playing positive roles in inhibiting tumor growth [4]. Although 5-FU-based therapy is widely used in the standard first-line treatment of malignant GC, unexpected gastrointestinal toxicity and drug resistance greatly limit its clinical application [5,6]. Biomarkers of gastric cancer have also been studied, but mechanism still needs further exploration and confirmatory research [7,8]. In brief, GC still has a poor prognosis, with a low 5-year survival rate for patients diagnosed at advanced stages of GC [9,10]. Therefore, it is urgent to design new GC treatments that enhance therapeutic effects and reduce toxicity in the treatment of GC.

The cumulative data show that cancer cell death involves induction of cell cycle arrest, apoptosis, and autophagy, suggesting a possible strategy to deal with gastric cancer [11,12]. At present, investigation of cell cycle has been widely performed and the arrest of cell cycle phase has been shown to be very effective in the inhibition of cell viability [13,14]. Apoptosis (type-I PCD) is a form of programmed cell death (PCD) that can be activated through 2 dominating signaling pathways, consisting of the extrinsic (death receptor pathway) and intrinsic (mitochondrial pathway) pathways [12]. In addition, apoptosis pathways also involve the B cell lymphoma-2 (Bcl-2) family proteins, which are divided into 2 groups of pro-apoptotic proteins (Bax, and Bak and Bad) and a third group of anti-apoptotic proteins (Bcl-2, Bcl-XL, and Mcl-1) [15]. Apart from the pro-survival effect of autophagy, autophagy can also facilitate cell death (type-II PCD) in some cell types under certain intensities of stimulation [16].

Usnic acid (UA, Figure 1A), a prominent secondary lichen metabolite, is abundant in various lichen species, including *Alectoria, Cladonia, Usnea, Lecanora, Ramalina, and Evernia*, being found in 2 enantiomeric forms: (–)-usnic acid and (+)-usnic acid [17]. Usnic acid has been used as an additive in cosmetics, toothpaste, and traditional medicines [18]. In the United States market, the sodium salt of usnic acid used to be sold as a dietary supplement to help control weight [18]. However, many cases of liver toxicities associated with chronic consumption of usnic acid were reported, causing withdrawal of the weight-loss drug [19]. Massive research was then carried out and demonstrated that usnic acid at high doses induces toxicity in Hepar cells and hepatotoxicity in animal models [20,21]. Aside from the toxicity, UA was reported to possess several biological and physiological properties, such as antiviral, antimicrobial, antiprotozoal, larvicide, UV protection, anti-inflammatory, antioxidation, healing, and antitumor activities [22]. Previous studies have demonstrated that UA can inhibit tumor activities (anti-proliferative, anti-angiogenesis, and inhibition of detachment and invasion) through different signaling pathways in various types of tumor cells, such as lung cancer cell lines (H1299, H1650, H1975, A549) [23,24], prostate cancer (CWR22Rv-1) [25], human ovarian carcinoma cell lines (A2780) [26], human colon adenocarcinoma cell lines (HT-29) [25,26], human gastric cancer cell lines (AGS) [25], and human breast cancer cell lines (MCF7, MDA-MB-231, Bcap-3) [27].

However, it is still not well-established that UA induces cell cycle arrest, cell apoptosis, and autophagy in GC cells *in vitro* and *in vivo*. Therefore, in the present study, we investigated the functional roles of UA with associated molecular alterations *in vitro* and in an *in vivo* xenograft tumor model.

Material and Methods

Chemicals and UA treatment, cell lines, and cell culture

(+)-usnic acid powder (UA, #329967, HPLC, purity ≥98%, Figure 1A) and 5-fluorouracil (5-FU, #F6627, HPLC, purity ≥99%) were obtained from Sigma-Aldrich. We prepared a 50-mM stock solution of UA (in DMSO) and a 50-mM solution of 5-FU (in DMSO) kept in the dark at –20°C, and then freshly diluted at required concentrations in cell culture medium or phosphate-buffered saline (PBS, #KGM20012) prior to use in each experiment. We used a 0.1% final concentration of DMSO as the control. In the cell viability assay, UA was added to prepared concentrations of 31.25, 62.5, 125, 250, 500, and 1000 µM for 24 and 48 h. For other experiments, assays were performed after 24 h of incubation of UA (BGC823: 100, 200, 400 µM; SGC7901: 300, 600, 1200 µM).

Human gastric carcinoma cell lines (BGC823 and SGC7901) were collected in our laboratory, obtained from the Cell Bank of the Shanghai Institute of Biochemistry and Cell Biology, Chinese Academy of Sciences (Shanghai, China), where they were tested and authenticated according to American Type Culture Collection standards. All cell lines used in the present study were maintained in RPMI-1640 medium (#GNM-23471, GENOM, Hangzhou, China), supplemented with 10% fetal bovine
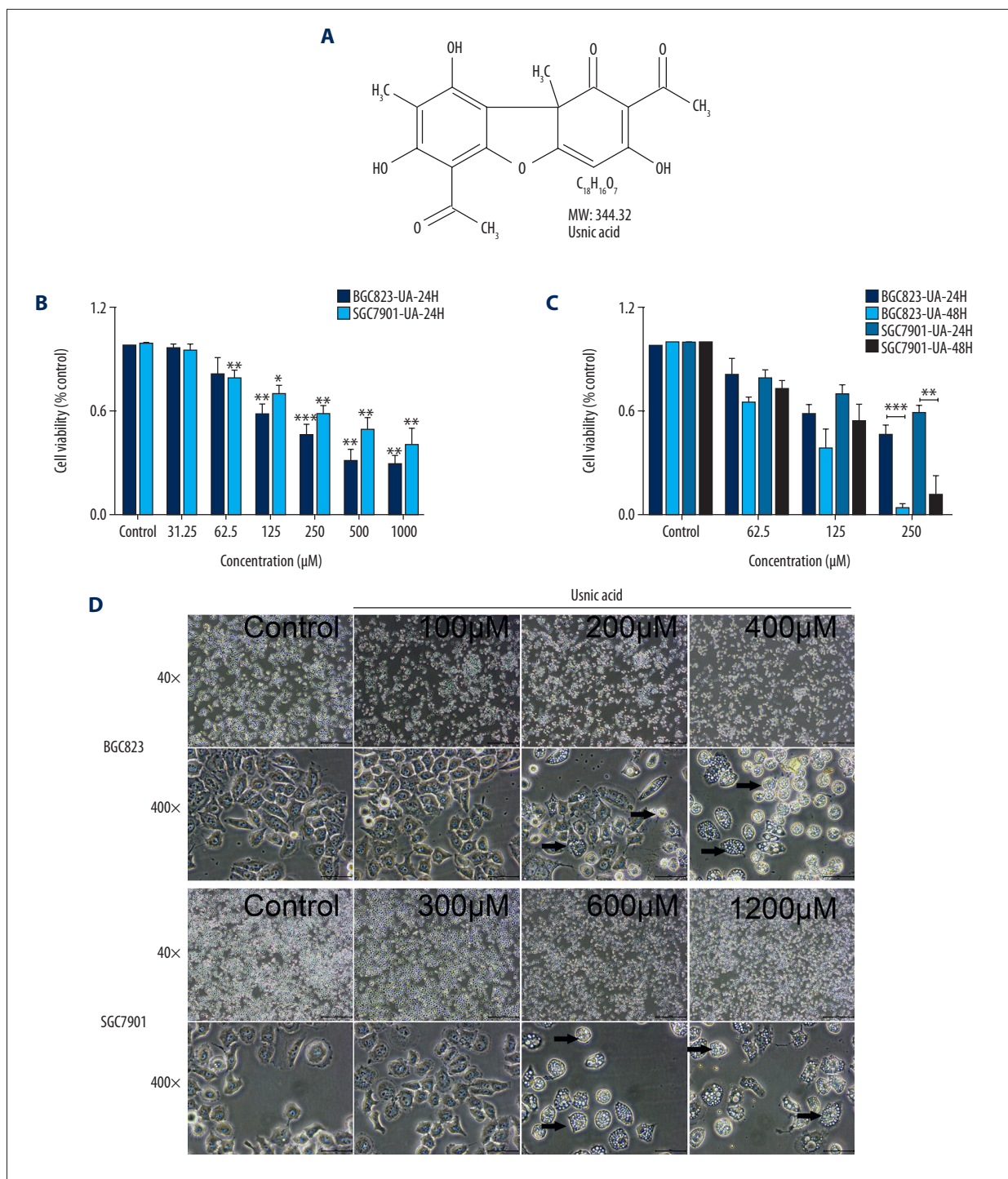
Figure 1. Effect of UA on cell proliferation (**B, C**) and the morphological changes (**D**) in BGC823 and SGC7901 cells. (**A**) The chemical structural formula of UA. (**B, C**) UA inhibited BGC823 and SGC7901 cells proliferation in a dose-dependent (**B**) and time-dependent (**C**) manner in a CCK8 assay. Cells were treated with various concentrations of UA (0.1%DMSO, 31.25, 62.5, 125, 250, 500, and 1000 μM) for 24 h and 48 h, followed by CCK8 measurement. The data represent the mean ±SD from 3 independent experiments with similar results. * $P<0.05$; ** $P<0.01$; *** $P<0.001$ (compared with control). (**D**) BGC823 and SGC7901 cells were treated with UA for 24 h and then observed under an optical microscope. Cells with an irregular shape in images are cells with morphological changes compared to control cells (black arrows). Lower magnification (40×) and higher magnification (400×) images.

serum (FBS, #04-001-1A/B, Biological Industries, Israel) and 1% penicillin/streptomycin mixture (#PS2004HY, Institute of Biomedical Engineering, Chinese Academy of Medical Sciences, Shanghai, China) at 37°C in a humidified atmosphere of 5% CO_2 and 95% air. Cells in the logarithmic growth phase were harvested from the culture flasks using 0.25% Trypsin/EDTA (#GNM27250, GENOM, Hangzhou, China), and centrifuged at 1000 rpm for 5 min, resuspended, and counted for use in subsequent experiments.

Cells viability assay by Cell Counting Kit-8 (CCK-8)

To assess the viability of the human GC cells treated with UA, the Cell Counting Kit-8 assay was performed according to the manufacturer's protocols. Briefly, BGC823 and SGC7901 cells were seeded into 96-well plates (6000–8000 cells/well) with a total volume of 100 µl medium per well, and allowed to attach for 24 h. Then, the cells were treated with a series of corresponding concentrations of UA (0–1000 µM) for 24 h and 48 h. At the end of incubation, the medium was removed, and the cells were treated with 10% CCK-8 (Dojindo Laboratories, Kumamoto, Japan) in 100 µl RPMI-1640 medium without FBS for 2 h in the dark at 37°C. We measured the absorbance of each well at 450 nm by using a microplate reader (ELX808; Bio Tek, Winooski, VT, USA) and the half-maximal inhibitory concentration (IC50) values were calculated using probit analysis of SPSS version 19.0. Cell viability was calculated according to the following formula: the viability ratio (%) =[(O1–O3)/(O2–O3)]×100, where O1 is the OD value of drug experimental group, O2 is the OD value of blank control group (0 µM of UA), and O3 is the OD value of the RPMI1640 medium without cells.

Cell morphology assay (Inverted Optical Microscopy)

We further observed the changes in cell behavior of UA-treated BGC823 and SGC7901 cells. Briefly, cells were plated in 6-well plates ($5×10^5$ cells per well). At 40–60% confluence, culture medium was replaced with fresh medium with various concentrations of UA, and then cells were incubated for a further 24 h. Cells morphological changes were observed by use of an inverted microscope (Olympus Corporation, USA).

Cell cycle analysis by flow cytometry

Flow cytometry (BD FACS Calibur™; Becton-Dickinson, Franklin Lakes, NJ, USA) was used to analyze the cell cycle distributions using the Cell Cycle Staining Kit (PI/RNase Staining Buffer #550825, BD Pharmingen, USA) according to the manufacturers' instructions. In brief, human GC cells were seeded in 6-well plates at a density of $5.0×10^5$ cells/well. After 24 h, the medium was removed and replaced with fresh medium containing a graded concentration of UA for another 24 h. The cells were then harvested and cell suspensions were pelleted and washed by centrifugation at 1000 rpm at 4°C. Cells were then fixed in cold 70% ethanol at –20°C overnight. After that, ethanol-fixed cells were centrifuged at 1000 rpm at room temperature and washed twice with cold PBS and FACS buffer. Then, single-cell suspensions at a density of $1×10^6$ of BGC823 or SGC7901 cells were resuspended in PI/RNase Staining Buffer and incubated for 15 min in the dark at room temperature and transferred to flow cytometry tubes for cell cycle analysis at slow flow rate and then analyzed in the ModFit LT5.0 program (*http://www.vsh.com/products/mflt/mfTrialVersions.asp*).

Cell cellular apoptosis assay by Hoechst staining

Hoechst33258 staining assay was used to evaluate cellular apoptosis. The procedure for Hoechst staining was carried out using Hoechst33258 (#C0003, Beyotime, Shanghai, China) kits according to the manufacturer's instructions. Briefly, cells in 6-well plates were exposed to UA for 24 h, then the GC cells were fixed for 10 min in 4% paraformaldehyde, washed in cold PBS, and incubated at room temperature for 5 min with Hoechst33258 in the dark. Stained cells were washed twice with PBS and then observed with a fluorescence microscope (Leica, Wetzlar, Germany) under UV excitation.

Western blotting

For Western blot analysis, cells were seeded in 6-well plates at a density of $1×10^6$ cells/well with 2 ml of culture medium. Following UA treatment with indicated concentrations for 24 h, cells were lysed in RIPA lysis buffer supplemented with a proteasome and phosphatase inhibitor (#P1049, Beyotime Institute of Biotechnology, China). The total protein was determined with a BCA protein assay kit (#P0010, Beyotime Institute of Biotechnology, Shanghai, China). Then, comparable amounts of protein were separated by 10% sodium dodecyl sulfate polyacrylamide gel electrophoresis and transferred to a polyvinylidene fluoride membrane (Millipore, Shanghai, China). After blocking with 5% nonfat dry milk for 1 h at room temperature, the PVDF membranes (Millipore, Billerica, Massachusetts, USA) were incubated overnight at 4°C with primary antibodies specific for glyceraldehyde-3-phosphate dehydrogenase (GAPDH) (1: 5000, Abcam, Cambridge, UK), Bax, Bcl-2, activated caspase3, PARP, cleaved PARP, P62, and LC3a/b (1: 1000; Cell Signaling Technology, Boston, USA). Horseradish peroxidase (HRP)-conjugated goat anti-rabbit Ig G (1: 1500; Cell Signaling Technology, Boston, USA) was applied as a secondary antibody for 2 h at room temperature. The immunoreactive bands were detected using an enhanced chemiluminescent detection reagent (Millipore, Shanghai, China). The immunoreactive bands were scanned by a Bio-Rad XRS chemiluminescence detection system (Bio-Rad, Hercules, CA, USA).

Animals and animal experiment

For *in vivo* evaluation, all animal experiments were conducted in accordance with the Guidelines for the Care and Use of Laboratory Animals of the Council of Science and Technology of China and approved by the Principles of Laboratory Animal Care of Zhejiang Chinese Medical University. Twenty-four 4-week-old female BALB/C nude mice (20±2g) were purchased from the Shanghai SLAC Laboratory Animal Co. Ltd (Shanghai, China) and maintained at the Experimental Animal Center of the Zhejiang Chinese Medical University. All mice were kept in a controlled environment with a 12-h phase shift in the light/dark cycle, room temperature of 24±1°C, and relative humidity of 50±10%, and had free access to autoclaved food and water. The BGC823 tumor cells were harvested during the growth phase, and suspended in sterile PBS ($1×10^7$ cells/mL). Cells were pipetted to single-cell suspensions, and each 100 μL solution was injected subcutaneously into the right flank of nude mice (0.1 mL, $1×10^6$ cells/mouse) to establish the malignant BGC823 tumor-bearing mouse model after feeding for 1 week. Tumor volume was measured with calipers once every 2 nights. About 1 week later, when the tumor size reached about 100 mm³, 24 mice were assigned randomly into control and experiment groups: control group (n=6); 5-FU (25 mg/kg) group (n=6); UA (100 mg/kg) group (n=6). Mice in control, 5-FU, and UA groups were injected with normal saline (i.p.), 5-FU (i.p.), and UA (i.p.) for 11 days (once every 2 days), respectively. The dosage of UA was based on the related research in the literature [27,28] and our pilot trial. In the process of drug administration, the weights of tumor-bearing mice and tumor diameters were recorded once every 2 days. One hour after the last treatment, the mice were killed humanely to collect the tumors. Tumor volumes were determined using the following formula: $V=0.5×L×W^2$, where, V is the volume, L is the length, and W is the width.

Histological assessment

The tumor tissues were cut and fixed using 4% paraformaldehyde for 24 h at room temperature and then dehydrated and embedded in paraffin. After deparaffination and rehydration, 2-μm-thick tissues were mounted on polylysine-coated slides for H&E staining. Images of H&E staining were obtained using a microscope. Using immunohistochemical method, the presence of Bax (#GB11007, Servicebio, 1: 300) and Bcl-2 (#GB11008, Servicebio, 1: 300) in the paraffin-embedded tumor tissues were assayed. Staining was performed as defined in the manufacturer's staining protocol. Samples were randomly selected from the tumor tissues. Immunostainings were performed with known positive and negative tumor controls. Immunohistochemical staining slides were scanned by a high-speed digital slide microscopy scanners-Panoramic MIDI with a 20× microscope objective (3DHISTECH, Hungary). Computer

analysis of staining intensity of IHC reaction image of all areas was performed and the number of stained pixels/area was quantified using the Densito Quant module (3DHISTECH, Hungary). An intensity score of 0 to 3 was assigned to the intensity of tumor cells (0, none; 1, weak; 2, intermediate; 3, strong). A proportional score was given by the estimated proportion of positive tumor cells in percentage. The expressions of Bax and Bcl-2 were assessed by H-score system. H-score (histochemistry score) was calculated using the following formula:

$$H\text{-score}=\sum (I×Pi)$$
= (percentage of cells of weak intensity ×1)
+ (percentage of cells of moderate intensity ×2)
+ (percentage of cells of strong intensity ×3)
(I = intensity of staining, Pi = percentage of stained tumor cells)

The maximum H-score could be 300, corresponding to 100% of cells with strong intensity.

Statistical analysis

Statistical analyses were performed using software SPSS version 19.0 (IBM, Armonk, NY, USA) and software Graph-Pad Prism version 7.0 (Windows, Graph-Pad Software, San Diego, California, USA, www.graphpad.com.). All *in vitro* experiments were performed independently at least in triplicate. Statistical significant differences were determined by a two-tailed *t* test when comparing 2 groups. P<0.05 was considered as statistically significant. Data are expressed as mean ± standard deviation (SD).

Results

UA induces the inhibition of cell proliferation.

In vitro antitumor capabilities of UA were evaluated using the CCK8 assays. Serially diluted UA solutions were added to BGC823 and SGC7901 cells and incubated for 24 h and 48 h. As shown in Figure 1B, 1C, cell viability decreased in a concentration-dependent and time-dependent manner when treated with UA. The IC50 (24h) of UA in BGC823 cells was 236.55±11.12 μM, which was significantly lower (P=0) than the IC50 (24 h, IC50=618.82×1.77 μM) of SGC7901 cells, suggesting that BGC823 cells were more sensitive than SGC7901 cells to UA.

UA induces cell morphological change.

By observation under an inverted microscope, we found that GC cells growth was significantly decreased at the experimental concentration of UA. After treatment with UA for 24 h, a reduction in cell volume, shrunken cytoplasm, extensive
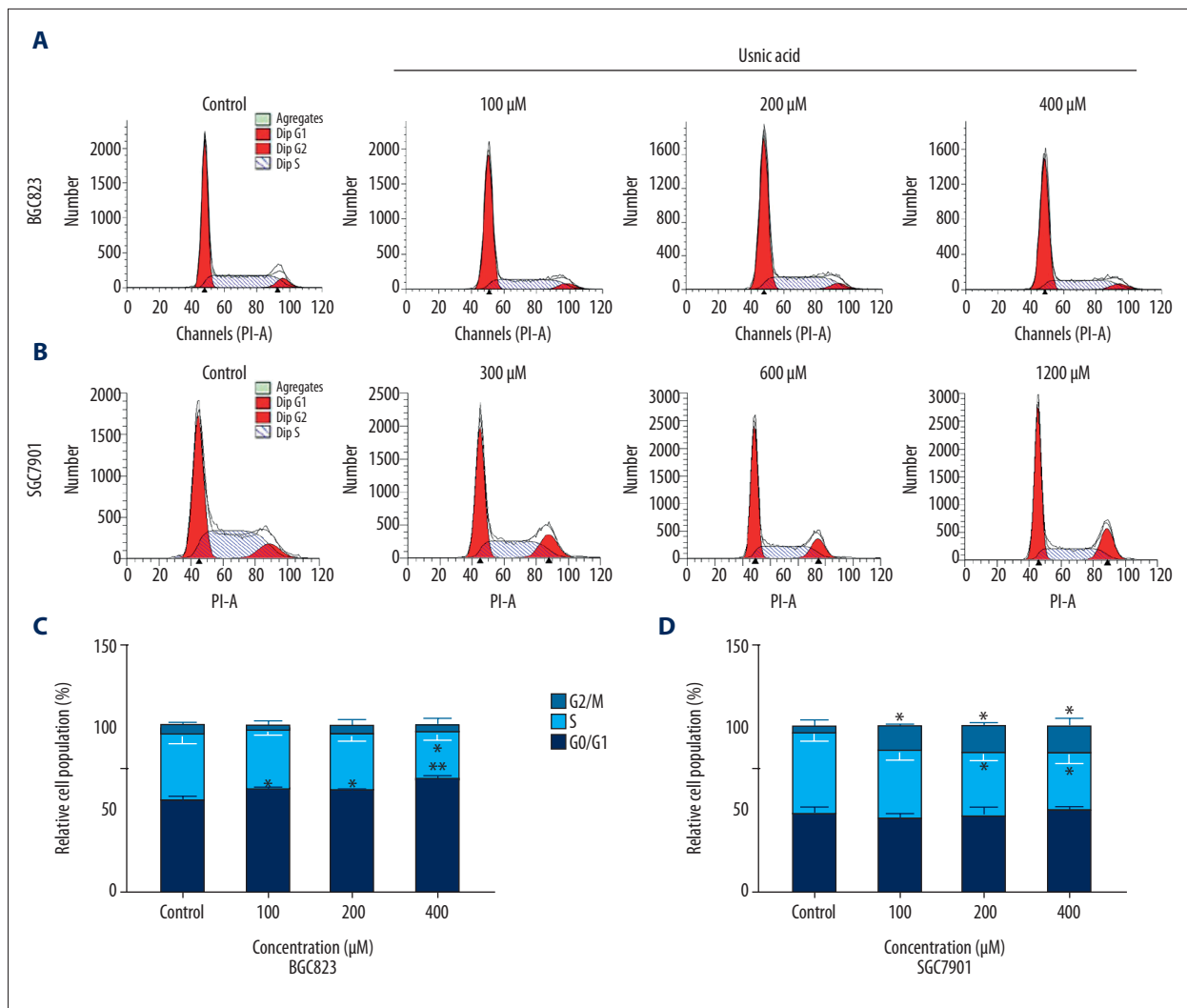
Figure 2. Effect of UA on cell cycle distribution in BGC823 (**A, C**) and SGC7901 (**B, D**) cells. (**A, B**) Cell cycle detection of BGC823 cells (**A**) and SGC7901 (**B**) cells following treatment with a graded concentration of UA for 24 h by flow cytometry. (**C, D**) Quantification of G0/G1, S, and G2/M phase cells in UA-treated BGC823 and SGC7901 cells at the indicated concentrations. The data represent the mean ±SD from 3 independent experiments. * P<0.05; ** P<0.01(compared with control).

vacuolization, and some cellular damage were observed, including most cells detached from culture surfaces, in a dose-dependent manner (Figure 1D, black arrows).

UA induces cell cycle arrest of G0/G1 or G2/M phase

To explore whether UA mediated the inhibition of GC cells growth via cell cycle arresting mechanisms, we analyzed cell cycle distribution subsequent to the cells being treated with indicated concentrations of UA for 24 h, using flow cytometry (PI staining). As shown in Figure 2, we found that UA treatment resulted in an accumulation of BGC823 cells in the G0/G1 phase from 54.4±2.7% to 66.9±2.6% (UA: 400 μM, P=0.005) and a significant decrease of BGC823 cells in the S phase

(P=0.043) from 39.7±4.7% to 28.7±4.5% as compared with the 0.1% DMSO control, and the effect was not dose-dependent (Figure 2A, 2C). UA exposure also induced an increase in G2/M phase cell population (from 4.7±3.9% to 16.7±4.4%, p=0.024, UA: 1200 μM) and a decrease in the S phase cell population (from 48.4±4.3% to 34.9±5.8%, p=0.031) in SGC-7901, and the effect was not dose-dependent (Figure 2B, 2D), suggesting that UA inhibited the growth of GC cells, partly resulting from inducing cell cycle arrest.

UA induces cell apoptosis and autophagy.

Chromatin condensation, a typical morphological change characteristic of apoptosis, was observed after Hoechst 33258
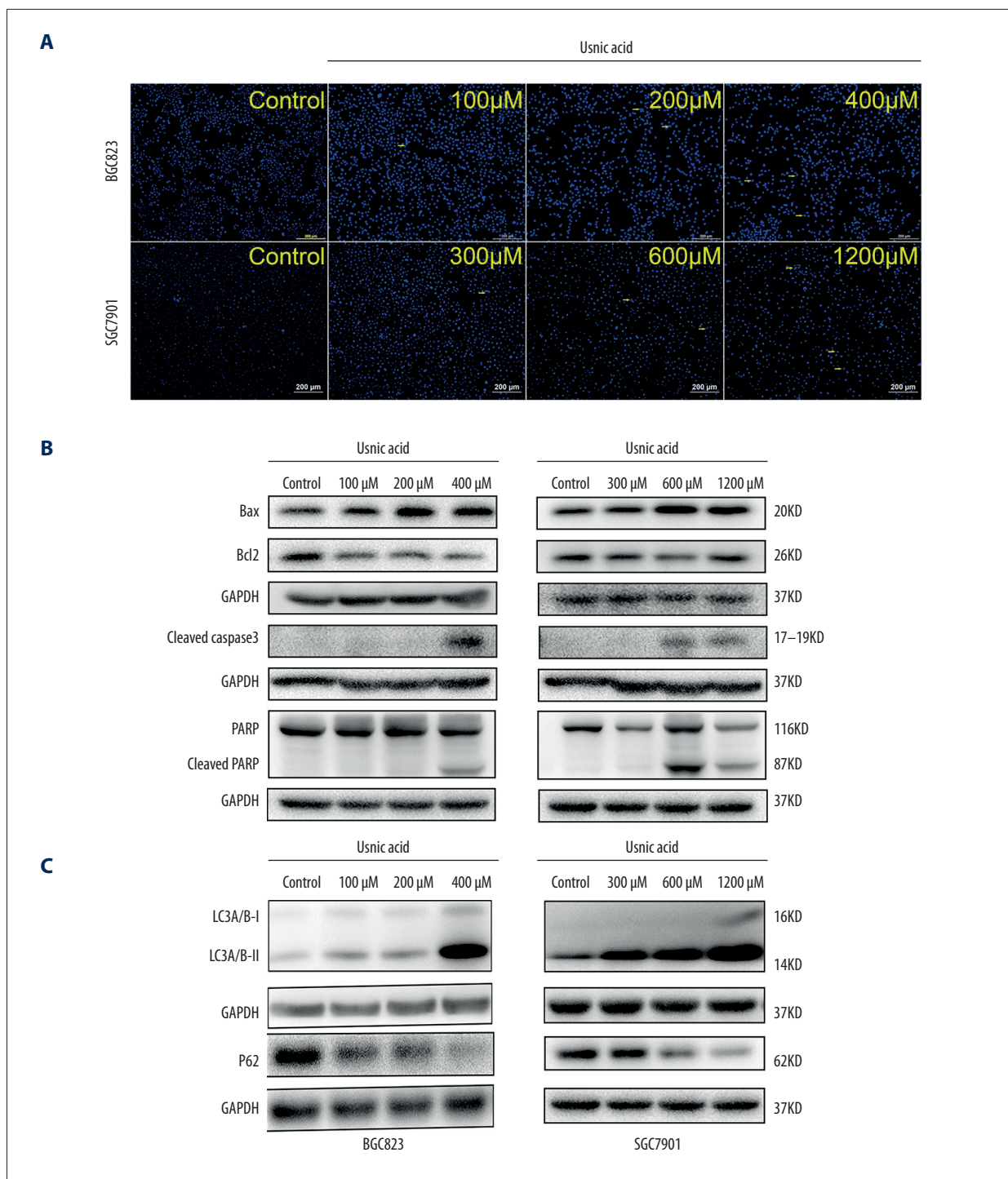
Figure 3. Usnic acid (UA) induces cell apoptosis and autophagy in gastric cancer. (**A**) Hoechst (blue) staining: representative morphology and apoptotic cells (yellow arrows) of BGC823 and SGC7901 cells treated with UA for 24 h. Original magnifications: 40× (**B**) Expression of Bax, Bcl-2, cleaved caspase-3, and cleaved PARP in BGC823 and SGC7901 cells treated with UA at the indicated concentrations for 24 h as assessed by Western blot. (**C**) Western blot analysis of main cellular autophagic markers in the BGC823 and SGC7901 cells treated with UA at the indicated concentrations. Data show a concentration – response up-regulation of LC3 and down-regulation of p62 in cells treated with UA as compared to control. GAPDH was used as an internal control. All experiments were repeated independently at least 3 times.
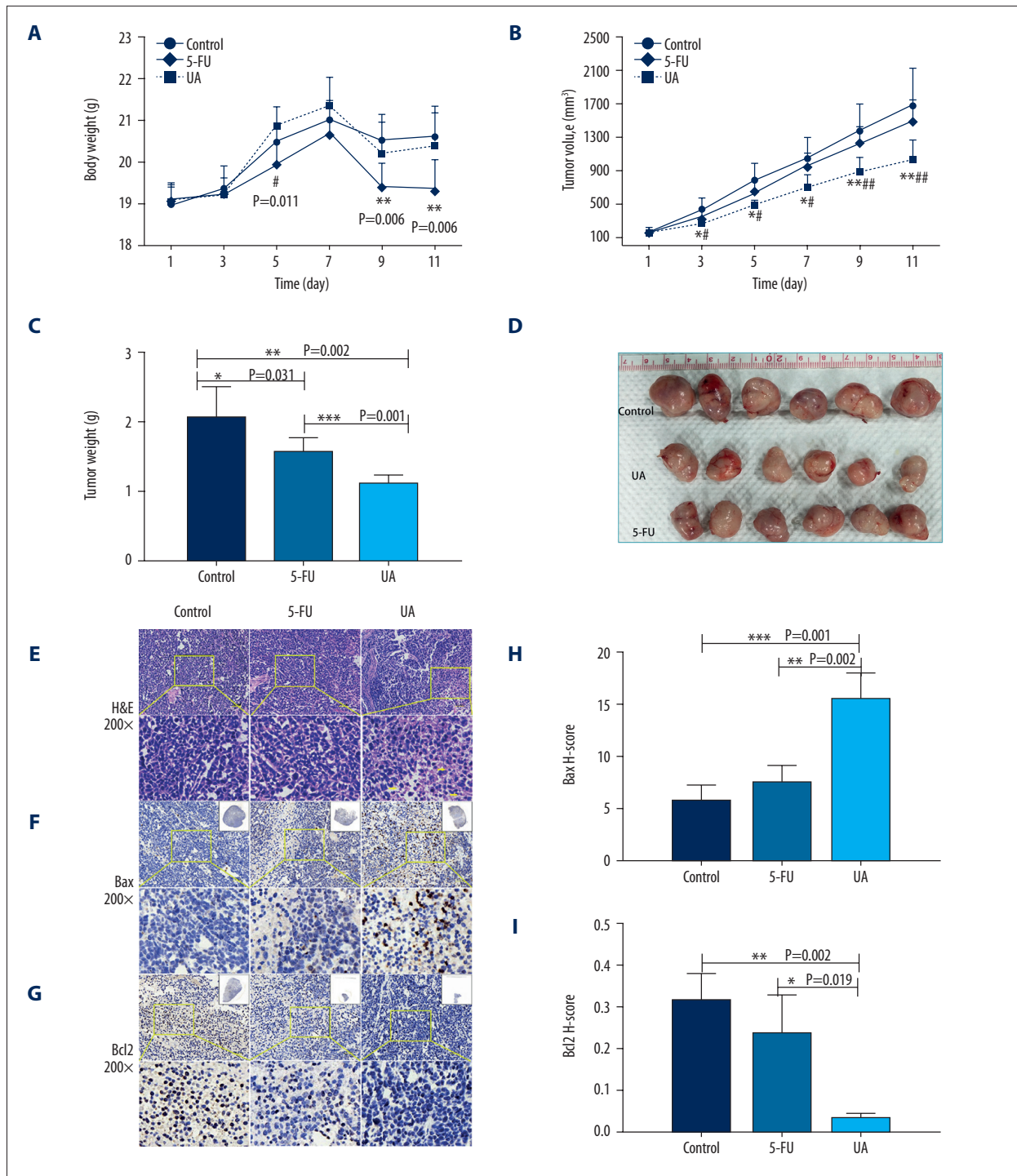
Figure 4. UA induces the suppression of tumor growth of BGC823-bearing nude mice. BGC823 cells were injected into the right flank of 5-week-old male nude mice. After injection of BGC823 cells, nude mice were treated with PBS, 5-FU (25 mg/kg), and UA (100 mg/kg) for 11 days. (**A**) Body weight changes of the mice during 11 days of treatment. # P<0.05 (UA compared with 5-FU), ** P<0.01 (control compared with 5-FU) (**B**) The tumor size of the xenograft tumors (''Materials and methods'' section). # P<0.05, ## P<0.01 (UA compared with 5-FU), * P<0.05, ** P<0.01 (UA compared with control). (**C**) Tumor weight changes of the mice during 11 days of treatment. * P<0.05, ** P<0.01, *** P<0.001. (**D**) The image of tumors. (**E–G**) Tumor tissues were examined by H&E staining (**E**, yellow arrow indicates necrotic cells) and immunohistochemical staining with Bax (**F**) and Bcl2 (**G**) antibodies. Original magnifications: 200×. (**H, I**) The mean value of the H-score of Bax (**H**) and Bcl2 (**I**). * P<0.05, ** P<0.01, *** P<0.001. All data represent the mean ±SD.

staining, while normal nucleus showed homogeneous staining. UA significantly increased the percentage of BGC823 cells and SGC7901 cells showing chromatin condensation (Figure 3A, yellow arrows). The possible signaling pathways through which UA induces cell apoptosis in GC cells were investigated. Western blot analysis revealed that the protein expression levels of Bax, activated caspase-3, and PARP were increased, but the level of Bcl-2 in GC cells was decreased, which led to cell apoptosis (Figure 3B). Some compounds have been demonstrated to induce autophagic cell death [29]; therefore, we decided to test whether UA could also induce the expression of autophagy-associated protein in GC cells. The bands showed that the protein expression levels of LC3-II and p62 were increased and decreased, respectively, in BGC823 and SGC7901 cells (Figure 3C).

UA induces the inhibition of tumor growth in BGC823-bearing mice

To assess the antitumor effect of UA *in vivo*, a BGC823 subcutaneous graft model was established. The weight of mice and the volume of tumors were positively correlated with the severity of tumors. There was no conspicuous difference in the weight and the tumor size among different groups prior to the drug treatment (P>0.05). As shown in Figure 4, the control group of animals with transplanted BGC823 cancer cells showed a progressive increase in their tumor volumes (Figure 4B) and tumor weight (Figure 4C, 4D). Compared to the control group, the tumor sizes (Figure 4B) and tumor weight (Figure 4C, 4D) of tumor-bearing mice in the UA group were significantly decreased (p<0.05) without weight loss (Figure 4A), while the decrease (P>0.05) in the 5-FU group was accompanied by weight loss (p<0.01) after the corresponding administrations. Moreover, UA administration was observed to exert a stronger antitumor effect on the tumor size and tumor weight compared to the 5-FU group (p<0.01). Therefore, UA treatment potentially attenuated side-effects of the agent and might be beneficial against GC cells.

UA induces the histopathological changes of tumor tissue.

As illustrated in Figure 4E–4I, the necrosis (yellow arrows) inside the tumor tissues (stained by H&E) showed the inhibitory efficacy of UA (Figure 4E). In immunohistochemistry (IHC) analysis for cell apoptosis, Bax-positive tumor cells were significantly increased after treatment with UA as compared to mice in the control and 5-FU groups (Figure 4F, 4H, p=0.001, p=0.002) while Bcl2-positive tumor cells were remarkably reduced after UA administration as compared to mice in the control and 5-FU groups (Figure 4G, 4I, p=0.002, p=0.019). These results show that UA exerted better antitumor growth as compared with control and 5-FU groups.

Discussion

Recently, usnic acid has been reported to exert an antitumor effect against various cancer cells by inducing cell cycle arrest, cell apoptosis, and autophagy, leading to the inhibition of cell proliferation and cell death [22. However, research on UA is still insufficient in GC cells. Therefore, in the present study, we examined the antitumor effects of UA in GC cell lines, as well as the underlying mechanisms, both *in vivo* and *in vitro*.

The present results indicate that UA inhibited the GC cell growth *in vitro* in a dose-dependent and time-dependent manner, using CCK-8 growth assay (Figure 1B, 1C). Uncontrolled proliferation resulting from abnormal activity of multifarious cell cycle proteins is a feature of cancer [30]. Data from cell cycle distribution assay by flow cytometry showed that UA induced G0/G1 or G2/M phase arrest in BGC-823 (Figure 2A, 2C) and SGC7901 (Figure 2B, 2D) cells with no dose-dependent response, making GC cells undergo apoptotic progression. This finding is similar to previous studies in which UA was revealed to induce G0/G1 phase arrest in human lung cancer [24] and G2/M phase arrest in human AGS cancer cells [25]. The Hoechst 33258 staining assay showed that treatment with UA also triggered cell apoptosis (Figure 3A). In addition, apoptosis and autophagy induced by UA were validated by measuring the level of apoptosis – (Figure 3B) and autophagy – (Figure 3C) associated proteins by Western blot. All these findings are consistent with previous studies showing that UA induces cell cycle arrest, apoptosis, and autophagy in some cells, including breast cancer and lung cancer [23,26]. All results mentioned above indicated that UA can suppress the proliferation of human GC cells by inducing cycle phase arrest, cell apoptosis, and autophagy.

Apoptosis is a type of cancer cell death and is considered a crucial target for cancer therapy [31]. Typically, activation of the extrinsic (death receptor-mediated) and the intrinsic (mitochondrial-mediated) pathways participate in the induction of cellular apoptosis [32]. In both apoptotic pathways, caspases (cysteinyl proteases family) are the key components, cleaving target proteins. Procaspase-8 is activated by membrane-associated protein complexes (Fas-L/TNF) in the extrinsic pathway, while procaspase-9 is activated by mitochondria-associated protein in the intrinsic pathway. Then, procaspase-3 is activated at the convergent point of the 2 pathways and the target proteins (PARP proteins) of cleaved caspase-3 are activated afterwards [33]. The present results revealed that UA treatment led to an increase of cleaved PARP and activated caspase-3, confirming that UA can induce apoptosis via activation of a caspase cascade. In addition, the BCL-2 family also plays major roles in apoptosis, covering anti-apoptosis protein (BH1-4 domains) and pro-apoptosis protein (BH1-3 and BH3 domains) [34]. Specifically, the Bcl-2 subfamily (Bcl-2, Bcl-xL, Bcl-w, Mcl-1, and A1/Bfl-1) is associated with the inhibition of

apoptosis, whereas the Bax subfamily (Bax, Bak, and Bok/Mtd) and the BH3-only subfamily (Bid, Bad, Bim/Bod, Bmf, Bik/Nbk, Blk, Noxa, Puma/Bbc3, and Hrk/DP5) promote apoptosis [35]. In the present study, UA treatment up-regulated the expression of pro-apoptotic protein Bax and down-regulated the expression of anti-apoptotic protein Bcl-2, suggesting the induction of apoptosis by UA in BGC-823 and SGC-7901 cells through regulating Bcl-2 family proteins. Previous studies revealed that UA induced apoptosis through the mitochondrial apoptotic pathways in cancer cells [26,27].

Autophagy is a low-level essential catabolic process of self-degradation and recycling of cellular constituents involving double-membraned vesicles and lysosomes [27]. This process can be accelerated in cancer cells under cellular stressors such as nutrient starvation, DNA damage, and organelle damage [36]. Although autophagy is considered a protective mechanism against ischemia in tumors, hyper-activation of autophagy can lead to cell death [37]. LC3 proteins, especially LC3-II, are recognized as the most common markers of autophagy, and P62 is incorporated in the completed autophagosomes and then degraded in autolysosomes [38,39]. The present study demonstrated that UA induced autophagy via the down-regulation of p62 and the up-regulation of LC3-II. A previous study showed that UA induces autophagic cell death in cells via inhibition of PI3K/AKT/mTOR [40].

The present study showed that UA suppressed the human GC cells (BGC823) tumor formation in the xenograft model *in vivo* (Figure 4). The mean tumor volume of UA-treated mice was smaller compared with controls (Figure 4B–4D). UA treatment reduced tumor burden and increased the number of necrotic cells inside the tumors, compared with tumors from PBS-treated mice (Figure 4E). Staining of apoptosis-associated proteins (Figure 4F–4I, Bax, Bcl2) confirmed the cells apoptosis by UA since the tumor cells in UA group had a significantly larger population of Bax and a smaller population of Bcl2-positive cells as compared to the PBS group. A previous study showed that the growth of lung cancer tumors was inhibited in UA-pretreated cancer cell xenografts inhibited at the dose of 10 μM [25]. The results of the present study are in agreement with those of some previous studies, including studies on hepatoma cells [28], and further illustrates that UA may also be used in different cancers.

Conclusions

In conclusion, results revealed that UA can induce autophagy and inhibit the proliferation of human GC cells *in vitro* by inducing phase arrest and cell apoptosis. UA treatment also has a better antitumor effect than 5-Fu *in vivo*. All data from the present study suggest that UA is an attractive and promising candidate for developing antitumor drugs targeting GC.

Conflicts of interest

None.

References:

1. Torre LA, Bray F, Siegel RL et al: Global cancer statistics, 2012. Cancer J Clin, 2015; 65(2): 87–108

2. Ychou M, Boige V, Pignon JP et al: Perioperative chemotherapy compared with surgery alone for resectable gastroesophageal adenocarcinoma: An FNCLCC and FFCD multicenter phase III trial. J Clin Oncol, 2011; 29(13): 1715–21

3. Thrumurthy SG, Chaudry MA, Chau I, Allum W: Does surgery have a role in managing incurable gastric cancer? Nat Rev Clin Oncol, 2015; 12(11): 676–82

4. Fontana E, Smyth EC: Novel targets in the treatment of advanced gastric cancer: A perspective review. Ther Adv Med Oncol, 2016; 8(2): 113–25

5. Bilici A: Treatment options in patients with metastatic gastric cancer: Current status and future perspectives. World J Gastroenterol, 2014; 20(14): 3905–15

6. Vazquez C, Orlova M, Angriman F et al: Prediction of severe toxicity in adult patients under treatment with 5-fluorouracil: A prospective cohort study. Anticancer Drugs, 2017; 28(9): 1039–46

7. Chen Y, Tian P, Liu Y: P53 and protein phosphorylation regulate the oncogenic role of epithelial cell transforming 2 (ECT2). Med Sci Monit, 2017; 23: 3154–60

8. Ye F, Jin P, Cai X et al: High RNA-binding motif protein 3 (RBM3) expression is independently associated with prolonged overall survival in intestinal-type gastric cancer. Med Sci Monit, 2017; 23: 6033–41

9. Marano L, Polom K, Patriti A et al: Surgical management of advanced gastric cancer: An evolving issue. Eur J Surg Oncol, 2016; 42(1): 18–27

10. Fukami Y, Kaneoka Y, Maeda A et al: Adjuvant hepatic artery infusion chemotherapy after hemihepatectomy for gastric cancer liver metastases. Int J Surg, 2017; 46: 79–84

11. Wiman KG, Zhivotovsky B: Understanding cell cycle and cell death regulation provides novel weapons against human diseases. J Intern Med, 2017; 281(5): 483–95

12. Nagata S, Tanaka M: Programmed cell death and the immune system. Nat Rev Immunol, 2017; 17 (5): 333–40

13. Lee HL, Lin CS, Kao SH, Chou MC: Gallic acid induces G1 phase arrest and apoptosis of triple-negative breast cancer cell MDA-MB-231 via p38 mitogen-activated protein kinase/p21/p27 axis. Anticancer Drugs, 2017; 28(10): 1150–56

14. Chen J: The cell-cycle arrest and apoptotic functions of p53 in tumor initiation and progression. Cold Spring Harb Perspect Med, 2016; 6(3): a026104

15. Kale J, Liu Q, Leber B, Andrews DW: Shedding light on apoptosis at subcellular membranes. Cell, 2012; 151(6): 1179–84

16. Liu Y, Levine B: Autosis and autophagic cell death: The dark side of autophagy. Cell Death Differ, 2015; 22 (3): 367–76

17. Ingolfsdottir K: Usnic acid. Phytochemistry, 2002; 61(7): 729–36

18. Luzina OA, Salakhutdinov NF: Biological activity of usnic acid and its derivatives: Part 1. Activity against unicellular organisms. Russ J Bioorganic Chem, 2016; 42(2): 115–32

19. Garcia-Cortes M, Robles-Diaz M, Ortega-Alonso A et al: Hepatotoxicity by dietary supplements: A tabular listing and clinical characteristics. Int J Mol Sci, 2016; 17(4): 537

20. Moreira CT, Oliveira AL, Comar JF et al: Harmful effects of usnic acid on hepatic metabolism. Chem Biol Interact, 2013; 203(2): 502–11

21. Liu Q, Zhao X, Lu X et al: Proteomic study on usnic-acid-induced hepatotoxicity in rats. J Agric Food Chem, 2012; 60(29): 7312–17

22. Araujo AA, de Melo MG, Rabelo TK et al: Review of the biological properties and toxicity of usnic acid. Nat Prod Res, 2015; 29(23): 2167–80

23. Yang Y, Nguyen TT, Jeong MH et al: Inhibitory activity of (+)-usnic acid against non-small cell lung cancer cell motility. PLoS One, 2016; 11(1): e0146575

24. Singh N, Nambiar D, Kale RK, Singh RP: Usnic acid inhibits growth and induces cell cycle arrest and apoptosis in human lung carcinoma A549 cells. Nutr Cancer, 2013; 65(Suppl. 1): 36–43

25. Nguyen TT, Yoon S, Yang Y et al: Lichen secondary metabolites in *Flavocetraria cucullata* exhibit anti-cancer effects on human cancer cells through the induction of apoptosis and suppression of tumorigenic potentials. PLoS One, 2014; 9(10): e111575

26. Backorova M, Jendzelovsky R, Kello M et al: Lichen secondary metabolites are responsible for induction of apoptosis in HT-29 and A2780 human cancer cell lines. Toxicol In Vitro, 2012; 26(3): 462–68

27. Song Y, Dai F, Zhai D et al: Usnic acid inhibits breast tumor angiogenesis and growth by suppressing VEGFR2-mediated AKT and ERK1/2 signaling pathways. Angiogenesis, 2012; 15(3): 421–32

28. Su ZQ, Liu YH, Guo HZ et al: Effect-enhancing and toxicity-reducing activity of usnic acid in ascitic tumor-bearing mice treated with bleomycin. Int Immunopharmacol, 2017; 46: 146–55

29. Lin SR, Fu YS, Tsai MJ et al: Natural compounds from herbs that can potentially execute as autophagy inducers for cancer therapy. Int J Mol Sci, 2017; 18(7): pii: E1412

30. Lapenna S, Giordano A: Cell cycle kinases as therapeutic targets for cancer. Nat Rev Drug Discov, 2009; 8(7): 547–66

31. Ou L, Lin S, Song B et al: The mechanisms of graphene-based materials-induced programmed cell death: A review of apoptosis, autophagy, and programmed necrosis. Int J Nanomedicine, 2017; 12: 6633–46

32. Abraha AM, Ketema EB: Apoptotic pathways as a therapeutic target for colorectal cancer treatment. World J Gastrointest Oncol, 2016; 8(8): 583–91

33. Ma Y, Zhu B, Yong L et al: Regulation of intrinsic and extrinsic apoptotic pathways in osteosarcoma cells following oleandrin treatment. Int J Mol Sci, 2016; 17(11): pii: E1950

34. Inoue-Yamauchi A, Jeng PS, Kim K et al: Targeting the differential addiction to anti-apoptotic BCL-2 family for cancer therapy. Nat Commun, 2017; 8: 16078

35. Birkinshaw RW, Czabotar PE: The BCL-2 family of proteins and mitochondrial outer membrane permeabilisation. Semin Cell Dev Biol, 2017; 72: 152–62

36. Kimmelman AC, White E: Autophagy and tumor metabolism. Cell Metab, 2017; 25(5): 1037–43

37. Shimizu S, Yoshida T, Tsujioka M, Arakawa S: Autophagic cell death and cancer. Int J Mol Sci, 2014; 15(2): 3145–53

38. Liu WJ, Ye L, Huang WF et al: p62 links the autophagy pathway and the ubiqutin-proteasome system upon ubiquitinated protein degradation. Cell Mol Biol Lett, 2016; 21: 29

39. Ichimura Y, Komatsu M: Selective degradation of p62 by autophagy. Semin Immunopathol, 2010; 32(4): 431–36

40. Ebrahim HY, Akl MR, Elsayed HE et al: Usnic acid benzylidene analogues as potent mechanistic target of rapamycin inhibitors for the control of breast malignancies. J Nat Prod, 2017; 80(4): 932–52